



CrossMark
click for updates

Cite this: *RSC Adv.*, 2015, 5, 50105

Free oxoanion theory for BaMgAl₁₀O₁₇:Eu²⁺ structure decomposition during alkaline fusion process

Yifan Liu,^a Shengen Zhang,^{*a} Hu Liu,^a De'an Pan,^a Bo Liu,^a Alex A. Volinsky^b and Cheinchi Chang^{cd}

The alkaline fusion process is a useful pretreatment for rare earth elements (REEs) recycling from blue phosphor (BaMgAl₁₀O₁₇:Eu²⁺, BAM), but the lack of basic theory affects the further development of the alkaline fusion process. Different substances (KOH, NaOH, Ca(OH)₂, NaCl, Na₂CO₃, and Na₂O₂) were chosen to react with BAM to explain the alkaline fusion process; only KOH, NaOH, Na₂CO₃, and Na₂O₂ can damage the BAM structure. The BAM alkaline fusion reactions share similar processes. Europium and magnesium ions were bonded with free oxoanion (OH⁻, CO₃²⁻, O₂²⁻) preferentially to escape from the BAM structure. The remaining structure of barium aluminate eventually decomposed into aluminate and BaCO₃ in air. Cations (Na⁺, K⁺) were introduced to bond with the aluminate ions to maintain the charge balance of the reaction system. Free Oxoanion Theory (FOAT) was summarized to elucidate the structure decomposition process of BAM. The variation principle of determined lattice energy was in agreement with the FOAT analysis results. FOAT is very beneficial for the REEs recycling mechanism and alkaline fusion technology theory.

Received 13th April 2015

Accepted 26th May 2015

DOI: 10.1039/c5ra06598d

www.rsc.org/advances

1 Introduction

Rare earth elements (REEs) are an important strategic resource that are widely used as functional materials due to their essential role in permanent magnets, lamp phosphors, catalysts, rechargeable batteries, *etc.*^{1,2} With the consumption of natural REEs resources, the world is confronted with the risk of REE supply shortage.³⁻⁶ The re-use and recycling of REEs from end-of-life rare earth goods is an efficient method to use the rare earth natural resources in a sustainable, circular economy.² Waste phosphor has been gaining more attention due to the large amounts of REEs in it.⁷⁻⁹ Eu²⁺ activated barium magnesium aluminate blue phosphor (BaMgAl₁₀O₁₇:Eu²⁺, BAM) is widely used for plasma display panels and fluorescent lamps due to its high efficiency and excellent color characteristics. It has become an important focus of research in the field of renewable rare earth resources.¹⁰⁻¹²

BAM can't be dissolved by either acid or alkali at room temperature because of its strong bond strength.¹³ The alkaline

fusion process is a useful pretreatment for REE recycling from BAM in manufacturing. Liu *et al.* developed the dual dissolution by hydrochloric acid (DHA) method of REE recycling from waste phosphor. In this method, the red phosphor (Y_{0.95}Eu_{0.05})₂O₃ was dissolved by acid leaching first, then green phosphor (Ce_{0.67}Tb_{0.33}MgAl₁₁O₁₉, CMAT) and blue phosphor (BaMgAl₁₀O₁₇:Eu²⁺) were decomposed by alkaline fusion with caustic soda. The total leaching rate of the rare earth elements was 94.6% by DHA, much higher than the 42% achieved by the traditional method.¹⁴ Wu *et al.* used Na₂O₂ the molten salt alkaline fusion process for recovering REEs from waste phosphors, and more than 99.9% REEs were recovered.¹⁵ The alkaline fusion process can effectively improve the REEs recycling rate; however, basic theory and research regarding alkaline fusion are almost lacking and many related scientific issues remain unclear.¹⁶

Detailed information about the crystal parameters of BAM is essential for understanding the alkaline fusion behavior of BAM. The structure of BaMgAl₁₀O₁₇:Eu²⁺, or β -alumina, has a space group of *P6₃/mmc* and can be described as consisting of two spinel blocks (MgAl₁₀O₁₆) separated by one mirror plane (BaO), as shown in Fig. 1.^{13,17} A europium atom is introduced into BAM as an interstitial atom, but the precise location of the europium atom in BAM is not yet known.¹⁸ The assumption that Eu atoms partially replace Ba atoms on the mirror plane of BAM is widely accepted.¹⁹ Zhang *et al.* discussed the phase transformation during the process of BAM alkaline fusion with NaOH, and elucidated the decomposition mechanisms of the

^aInstitute for Advanced Materials & Technology, University of Science and Technology Beijing, Beijing 100083, P. R. China, +86-10-6233-3375. E-mail: zhangshengen@mater.ustb.edu.cn; Tel: +86-10-6233-3375

^bDepartment of Mechanical Engineering, University of South Florida, Tampa, FL 33620, USA

^cDepartment of Chemical, Biochemical, and Environmental Engineering, University of Maryland, Baltimore, MD 21250, USA

^dDepartment of Engineering and Technical Services, District of Columbia Water and Sewer Authority, Washington, DC 20032, USA

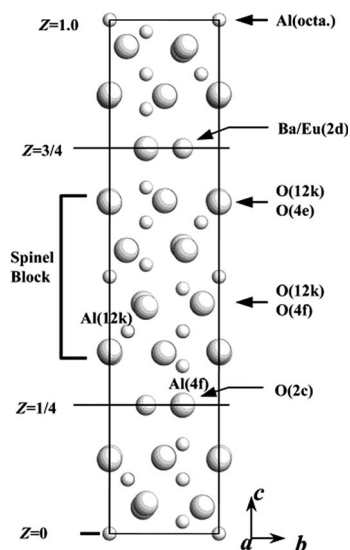


Fig. 1 Projection of the unit cells of the BAM crystal structure on the [110] plane.

BAM crystal structure.²⁰ Until now, no papers have reported the alkaline fusion process from the viewpoint of ions. Understanding the BAM structure decomposition will benefit the REEs recycling mechanism a lot, and the related theory can supplement the alkaline fusion technology theory.

In this paper, a series of alkaline fusion experiments of BAM powders were performed with six different reactants to separately elucidate the BAM structure decomposition during the alkaline fusion process. The BAM transformation in the alkaline fusion process was studied by thermal and X-ray diffraction (XRD) analyses. The lattice energy of the products was also determined to explain the smelt properties in the alkaline fusion process. By discussing these different BAM alkaline fusion reactions, a new theory, the Free Oxoanion Theory (FOAT), was put forward to elucidate the structure decomposition process of BAM.

2 Experimental

2.1 Materials and methods

The BAM powder used in this study was obtained from the Dalian Luminglight Co. in Liaoning Province, China. The powder has a particle size of 2–4 μm . The main phase is $\text{Ba}_{0.95}\text{Mg}_{0.912}\text{Al}_{10.088}\text{O}_{17}$ (PDF 84-0818) when detected by XRD. Six different reactants (KOH, NaOH, $\text{Ca}(\text{OH})_2$, NaCl, Na_2CO_3 , and Na_2O_2) were chosen to react with BAM. BAM powder was mixed with KOH, NaOH, $\text{Ca}(\text{OH})_2$, NaCl and NaCO_3 at a BAM/reactant mass ratio of 1 : 1 by ball-milling, while BAM was mixed with Na_2O_2 at a 1 : 1.5 mass ratio by ball-milling. Under this BAM/reactant mass ratio condition, BAM would be decomposed completely if the reaction could happen.

The mixtures of BAM and KOH were placed into 200 mL nickel crucibles, and the fusion was performed in a furnace at 150 $^\circ\text{C}$, 250 $^\circ\text{C}$, 300 $^\circ\text{C}$, 350 $^\circ\text{C}$, 400 $^\circ\text{C}$ and 450 $^\circ\text{C}$ for 2 hours. After the reaction, the crucibles were immediately placed in

water to cool the products. Then, all the fusion products were cleaned with deionized water several times at 60 $^\circ\text{C}$ under stirring (200 rpm) for 20 minutes. After filtration, the products were dried and ground to a size smaller than 52 μm (270 mesh) for XRD analysis.

The chosen reaction temperature parameters for different reactants are listed in Table 1. All mixtures were mixed for 2 hours. The “wash” behind the reaction temperature means that the fusion products were cleaned with deionized water several times by the method mentioned before. In order to exclude the effect of BAM structure change under high temperature, pure BAM was treated at 300 $^\circ\text{C}$, 600 $^\circ\text{C}$ and 900 $^\circ\text{C}$ for 2 hours. All products were analyzed by XRD, as for the mixtures of BAM and KOH.

XRD analysis was performed using a Philips APD-10 X-ray diffractometer with Cu $\text{K}\alpha$ radiation, 40 kV voltage and 150 mA current at 10°min^{-1} scanning rate, from 10° to 100° (2 theta angle range). Differential scanning calorimetry (DSC) and thermogravimetric (TG) analysis were carried out using a QUANTA 250 thermal analyzer. The reference material was α - Al_2O_3 powder, and the samples (74 μm) were heated from room temperature (RT) to 1000 $^\circ\text{C}$ at the heating rate of 10 $^\circ\text{C} \text{min}^{-1}$.

2.2 Lattice energy evaluation

Crystal lattice energies are important in considering the stability of materials, and the lattice energy reflects the natural tendency towards the organization of matter.^{21,22} The Bonn formula (eqn. (1)) is still widely accepted as an effective method to calculate ionic crystal lattice energy:

$$U = \frac{NaW_1W_2e^2}{d_0} \left(1 - \frac{1}{m}\right) \quad (1)$$

where U is the lattice energy, kJ mol^{-1} ; W_1 and W_2 are the electrovalues of the two ions; e is the electron charge ($1.602 \times 10^{-19} \text{ C}$); N is the number of 1 mol ionic crystal molecules (Avogadro constant, $6.02 \times 10^{23} \text{ mol}^{-1}$); a is the Madelung constant; d_0 is the balance distance between the positive and negative ions; and m is the Bonn index.

Scientist Kapustinskii improved the Bonn formula to get the Kapustinskii formula, where n is the number of ions:

$$U = \frac{287.2nW_1W_2}{d_0} \left(1 - \frac{0.345}{d_0}\right) \quad (2)$$

Table 1 Reaction temperatures used for different reactants

Reactants	Reaction temperature ($^\circ\text{C}$)
Pure BAM	300, 600, 900
BAM + KOH	150 wash, 250 wash, 300 wash, 350 wash, 400 wash, 450 wash
BAM + NaOH	150, 200, 250, 300 wash, 325 wash, 350 wash, 375 wash
BAM + $\text{Ca}(\text{OH})_2$	450, 650, 700, 800, 900
BAM + NaCl	400, 810
BAM + Na_2CO_3	400, 500, 600, 700, 800, 850, 900
BAM + Na_2O_2	300, 400, 500, 600, 700 wash

Table 2 Energy constants (EC, kJ mol⁻¹) of some ions

Monovalence	EC	Divalence	EC	Trivalence	EC	Negative	EC
K	0.36	Ba	1.36	La	3.58	Cl ⁻	0.25
Na	0.45	Ca	1.75	Y	3.95	O ²⁻	1.55
		Mg	2.15	Sc	4.65	OH ⁻	0.37
				Al	4.95	CO ₃ ²⁻	0.78
						AlO ₄ ⁵⁻	4.0

Both Bonn and Kapustinskii formulas can only be used for binary compounds. Based on these two formulas, Phil Mann refined the formulas to calculate the lattice energy of complex compounds:²³

$$U = 256.1 \times (n_1 EC_1 + n_2 EC_2 + \dots) \quad (3)$$

where n_1 and n_2 are the number of positive and negative ions in the unit cell; EC_1 and EC_2 are the energy constants of the ions.

Some energy constants of the correlative ions in this paper are listed in Table 2.

3 Results and discussion

3.1 Thermal analysis

The DSC results of all different mixtures are shown in Fig. 2. When BAM reacted with KOH, as shown in Fig. 2(a), there were two obvious endothermic peaks at 100 °C and 140 °C. The peak at 100 °C is mainly due to the evaporation of water, and this phenomenon is often observed in many other endothermic reactions, such as alkaline hydrolysis and thermal decomposition.^{24,25} The peak at 140 °C is mainly due to the CO₂ absorbed in KOH when the DSC sample was exposed to air. Between 100 °C and 200 °C, the sample had nearly 60% mass loss, which is consistent with moisture evaporation of the mixtures. An obvious endothermic peak was also observed at 235 °C, and it could be concluded that the BAM structure changed from this

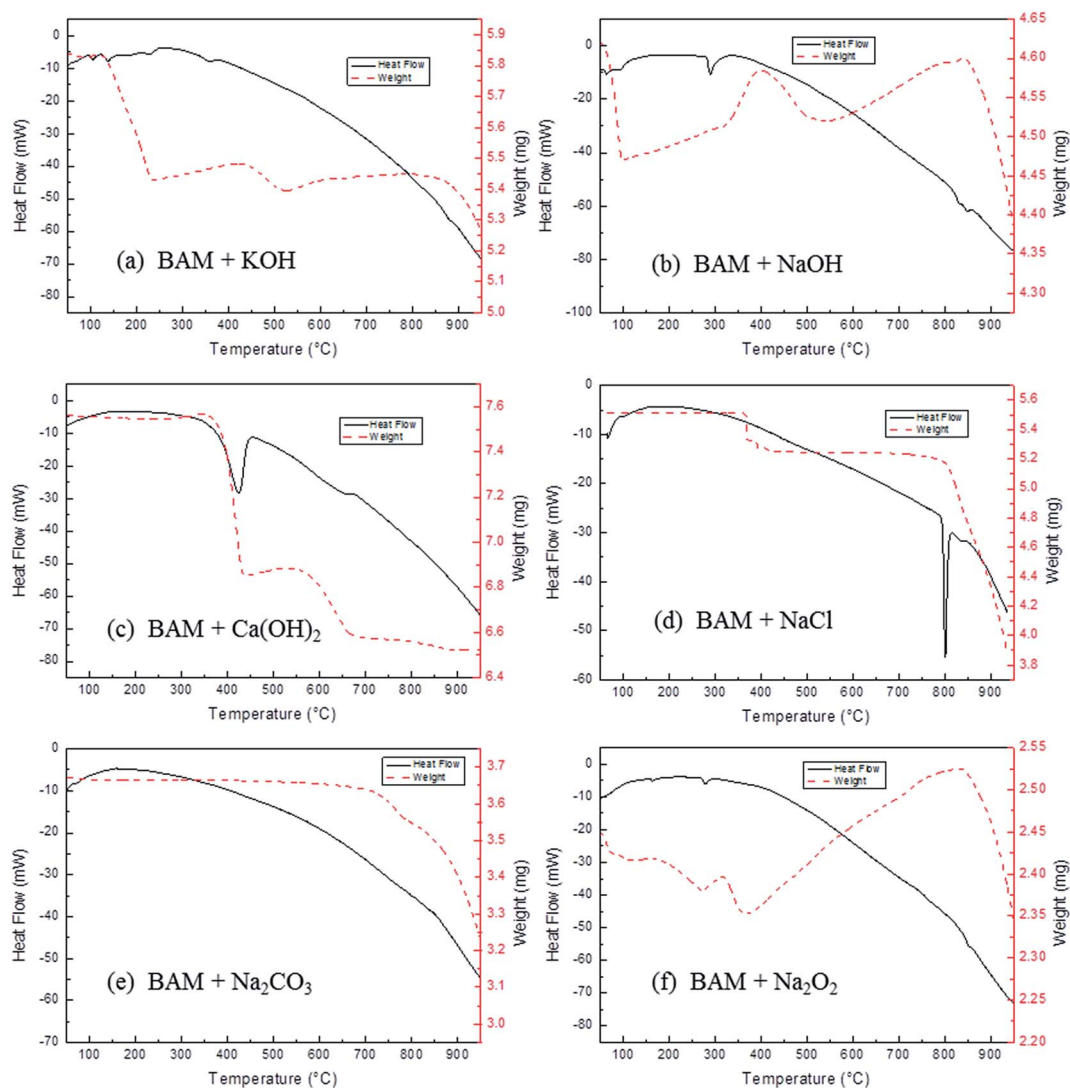


Fig. 2 DSC results of BAM alkaline fusion with different reactants (heating rate is 10 °C min⁻¹ in air); the downward heat flow peak means endothermic.

temperature. The BAM reaction could produce new products, and these products may react with the H₂O and CO₂ in air during the heating process. So after 250 °C, some endothermic peak and mass fluctuation could be observed in Fig. 2(a).

The DSC result of BAM reaction with NaOH, shown in Fig. 2(b), shares a similar trend with Fig. 2(a). Two obvious endothermic peaks were observed at 70 °C and 100 °C, which are mainly due to the moisture and CO₂ absorbed in NaOH. The endothermic peak observed at 290 °C shows that the BAM alkaline fusion reaction with NaOH began at about 290 °C. After 300 °C, an obvious mass fluctuation could be observed, which is mainly due to the further reaction of BAM reaction products during the heating process.

The DSC result of the BAM reaction with Ca(OH)₂ is shown in Fig. 2(c). A strong endothermic peak was observed at nearly 450 °C, and a possible explanation for this peak is that Ca(OH)₂ decomposed into CaO and H₂O from this temperature, while BAM remained the same. The sample had nearly 70% mass loss between 400 °C and 500 °C, which correlates to the decomposition of Ca(OH)₂. There is still a mass loss between 500 °C to 650 °C. In this period, Ca(OH)₂ decomposed completely. The DSC result of the reaction of BAM with NaCl is shown in Fig. 2(d). Neither an obvious heat flow change nor a mass change were detected simultaneously before 800 °C. The melting point of NaCl is 801 °C. There was a very strong and narrow endothermic peak at 800 °C, accompanied by a huge mass loss. All the details indicate that NaCl started to melt and evaporate when the temperature was higher than 800 °C, while BAM remained the same.

The DSC result of the reaction of BAM with Na₂CO₃ is shown in Fig. 2(e). The whole process was mild, and not much heat flow and mass change were detected. The behavior of BAM and Na₂CO₃ was temporarily unclear. The DSC result of the reaction of BAM with Na₂O₂ is shown in Fig. 2(f). An endothermic peak was observed at 290 °C, accompanied by some fluctuations. This indicates that the mixture will react at around 290 °C. There is an obvious mass fluctuation after 300 °C, which is mainly due to the further reaction of BAM reaction products during the heating process.

From the DSC results analysis, it could be concluded that Ca(OH)₂ and NaCl can't react with BAM up to 1000 °C. KOH, NaOH and Na₂O₂ exhibited strong alkaline properties to make the BAM structure decompose. By comparing the reaction endothermic peak and mass loss, the reaction between BAM and KOH and the reaction between BAM and NaOH followed a similar path, while both reactions were stronger than the reaction between BAM and Na₂O₂. The reaction between BAM and Na₂CO₃ was a mild process, and the reaction mechanism needs to be described by other means, which will be explained by the phase analysis.

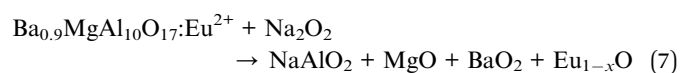
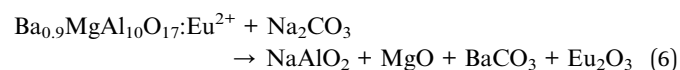
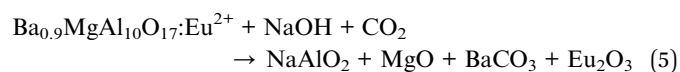
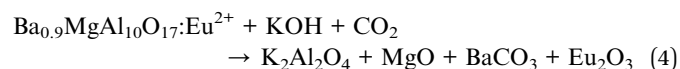
3.2 Phase analysis

The main phases of BAM reaction products with different reactants are listed in Table 3. The number behind every phase is the PDF number from the JADE software. The phase in

brackets means that this phase is lost in products because of the washing process. RT stands for room temperature in Table 3.

Due to thermal expansion, pure BAM (PDF 84-0818) partly transformed to Ba_{0.9}Eu_{0.1}Mg₂Al₁₆O₂₇ (PDF 50-0513) when heated, but the main structure remained unchanged. No phase change was detected in the reaction of BAM and NaCl, which indicates that NaCl can't damage BAM crystal structure in the studied temperature range. This result is consistent with DSC analysis. In the reaction between BAM and Ca(OH)₂, CaO (PDF 77-0210) can be detected from 450 °C, but when the reaction temperature was higher, Ca(OH)₂ (PDF 44-1481) disappeared, while the BAM phase had not changed. It is appropriate to explain the DSC trend for BAM reaction with Ca(OH)₂ corresponding to the phase analysis.

According to the phases listed in Table 3, KOH, NaOH, Na₂CO₃ and Na₂O₂ can damage the BAM structure to produce new substances through corresponding reaction eqn (4)–(7). The XRD data for these four reactions at different temperature are shown in Fig. 3. The BAM diffraction peak was slight split and shifted in Fig. 3(a–d), signifying the BAM crystalline size growth and phase transformation. Depending on comprehensive DSC and XRD analysis, the reaction mechanism for reactions (4)–(7) can be simply expressed by the flow diagram shown as Fig. 4.



By comparing these four flow diagrams in Fig. 4, it's clear that the BAM structure damage shares similar processes. Within the temperature range studied, Mg ions in BAM are bonded with free oxoanions (OH⁻, CO₃²⁻, O₂²⁻) preferentially to escape from the BAM structure, eventually forming stable MgO. In order to maintain the stability of the structure, Ba, Al and O ions can form a new structure of barium aluminate, such as BaAl₁₂O₁₉ (PDF 26-0315). As the reaction temperature increases, Ba ions are bonded with free oxoanion and eventually appear in the form of BaCO₃ in air. In the process of Ba and Mg ion extraction from the BAM structure, Na/K ions are diffused into the structure to bond with the aluminate ion to maintain the charge balance of the reaction system. The produced aluminate finally transforms into NaAlO₂/K₂Al₂O₄.

The europium content in BAM is small, thus only when BAM is substantially decomposed could europium-containing products be detected, and Fig. 3 reflects this phenomenon. In the BAM structure the europium atom is considered an interstitial atom, so its path has great uncertainty during the reaction

Table 3 Main phases of different BAM reactions

Reactants	T/°C	Main phase
Pure BAM	RT	Ba _{0.956} Mg _{0.912} Al _{10.088} O ₁₇ (84-0818)
	300/600/900	Ba _{0.956} Mg _{0.912} Al _{10.088} O ₁₇ (84-0818), Ba _{0.9} Eu _{0.1} Mg ₂ Al ₁₆ O ₂₇ (50-0513)
BAM + NaCl	RT	Ba _{0.956} Mg _{0.912} Al _{10.088} O ₁₇ (84-0818)
	400/810	Ba _{0.956} Mg _{0.912} Al _{10.088} O ₁₇ (84-0818), NaCl (77-2064)
BAM + Ca(OH) ₂	RT	Ba _{0.956} Mg _{0.912} Al _{10.088} O ₁₇ (84-0818)
	450	Ba _{0.956} Mg _{0.912} Al _{10.088} O ₁₇ (84-0818), Ba _{0.9} Eu _{0.1} Mg ₂ Al ₁₆ O ₂₇ (50-0513), Ca(OH) ₂ (44-1481), CaO (77-0210)
	650/700/800/900	Ba _{0.956} Mg _{0.912} Al _{10.088} O ₁₇ (84-0818), Ba _{0.9} Eu _{0.1} Mg ₂ Al ₁₆ O ₂₇ (50-0513), CaO (77-0210)
BAM + KOH	RT/150 wash	Ba _{0.956} Mg _{0.912} Al _{10.088} O ₁₇ (84-0818)
	230 wash	Ba _{0.956} Mg _{0.912} Al _{10.088} O ₁₇ (84-0818), Ba _{0.9} Eu _{0.1} Mg ₂ Al ₁₆ O ₂₇ (50-0513)
	300 wash/350 wash	Ba _{0.956} Mg _{0.912} Al _{10.088} O ₁₇ (84-0818), Ba _{0.9} Eu _{0.1} Mg ₂ Al ₁₆ O ₂₇ (50-0513), BaAl ₁₂ O ₁₉ (26-0135), MgO (77-2179), BaCO ₃ (41-0373), (K ₂ Al ₂ O ₄)
	400 wash	Ba _{0.956} Mg _{0.912} Al _{10.088} O ₁₇ (84-0818), MgO (77-2179), BaCO ₃ (41-0373), Eu ₂ O ₃ (34-0392), (K ₂ Al ₂ O ₄)
	450 wash	MgO (77-2179), BaCO ₃ (41-0373), Eu ₂ O ₃ (34-0392), (K ₂ Al ₂ O ₄)
	RT	Ba _{0.956} Mg _{0.912} Al _{10.088} O ₁₇ (84-0818)
BAM + NaOH	150/200/250	Ba _{0.956} Mg _{0.912} Al _{10.088} O ₁₇ (84-0818), Ba _{0.9} Eu _{0.1} Mg ₂ Al ₁₆ O ₂₇ (50-0513)
	300 wash/325 wash	Ba _{0.956} Mg _{0.912} Al _{10.088} O ₁₇ (84-0818), Ba _{0.9} Eu _{0.1} Mg ₂ Al ₁₆ O ₂₇ (50-0513), BaAl ₁₂ O ₁₉ (26-0315), MgO (87-0651), BaCO ₃ (05-0378), (NaAlO ₂)
	350 wash	Ba _{0.956} Mg _{0.912} Al _{10.088} O ₁₇ (84-0818), BaAl ₁₂ O ₁₉ (26-0315), MgO (87-0651), BaCO ₃ (05-0378), Eu ₂ O ₃ (34-0392), (NaAlO ₂)
	375 wash	MgO (87-0651), BaCO ₃ (05-0378), Eu ₂ O ₃ (34-0392), (NaAlO ₂)
BAM + Na ₂ CO ₃	RT	Ba _{0.956} Mg _{0.912} Al _{10.088} O ₁₇ (84-0818)
	400	Ba _{0.956} Mg _{0.912} Al _{10.088} O ₁₇ (84-0818), Ba _{0.9} Eu _{0.1} Mg ₂ Al ₁₆ O ₂₇ (50-0513), Na ₂ CO ₃ (37-0451)
	500	Ba _{0.956} Mg _{0.912} Al _{10.088} O ₁₇ (84-0818), Ba _{0.9} Eu _{0.1} Mg ₂ Al ₁₆ O ₂₇ (50-0513), Na ₂ CO ₃ (37-0451), BaAl ₁₂ O ₁₉ (26-0135), BaMg(CO ₃) ₂ (74-1492), Na ₂ Al ₂₂ O ₃₄ (31-1263)
	600/700	Ba _{0.956} Mg _{0.912} Al _{10.088} O ₁₇ (84-0818), Ba _{0.9} Eu _{0.1} Mg ₂ Al ₁₆ O ₂₇ (50-0513), Na ₂ CO ₃ (37-0451), BaAl ₁₂ O ₁₉ (26-0135), MgO (78-0430), Na ₂ Al ₂₂ O ₃₄ (31-1263)
	800	Ba _{0.956} Mg _{0.912} Al _{10.088} O ₁₇ (84-0818), Na ₂ CO ₃ (37-0451), BaAl ₂ O ₄ (72-1331), MgO (78-0430), Eu ₂ O ₃ (74-1988), Na ₂ Al ₂₂ O ₃₄ (31-1263)
	850	Ba _{0.956} Mg _{0.912} Al _{10.088} O ₁₇ (84-0818), Na ₂ CO ₃ (37-0451), BaCO ₃ (45-1471), MgO (78-0430), Eu ₂ O ₃ (74-1988), NaAlO ₂ (83-0316)
BAM + Na ₂ O ₂	900	Na ₂ CO ₃ (37-0451), BaCO ₃ (45-1471), MgO (78-0430), Eu ₂ O ₃ (74-1988), NaAlO ₂ (83-0316)
	RT	Ba _{0.956} Mg _{0.912} Al _{10.088} O ₁₇ (84-0818)
	300	Ba _{0.956} Mg _{0.912} Al _{10.088} O ₁₇ (84-0818), Ba _{0.9} Eu _{0.1} Mg ₂ Al ₁₆ O ₂₇ (50-0513), Na ₂ O ₂ (74-0111), BaO ₂ (07-0233), MgO ₂ (76-1363), Na ₂ Al ₂₂ O ₃₄ (72-1406), Na ₂ CO ₃ (77-2082)
	400	Na ₂ O ₂ (74-0111), Ba ₃ Al ₂ O ₆ (83-0468), BaO ₂ (73-1739), MgAl ₂ O ₄ (47-0254), MgO (75-1525), Na ₁₄ Al ₁₄ O ₁₃ (77-0095), Na ₂ CO ₃ (77-2082)
	500/600 700 wash	Na ₂ O ₂ (74-0111), BaO ₂ (73-1739), MgO (75-1525), NaAlO ₂ (83-0316), Eu _{1-x} O (17-0779), Na ₂ CO ₃ (77-2082), BaCO ₃ (71-2394), MgO (77-2364)

process. Zhang *et al.* found that in the process of BAM reaction with sodium hydroxide, europium ions were most likely to be replaced by sodium ions first and then leave the BAM structure, based on the oxygen atoms ratio analysis.²⁰ This result is consistent with the nature of interstitial atoms. In this paper it's also considered that europium was first bonded with free anions and then left the BAM structure.

By analyzing the BAM reaction behavior with NaCl, NaOH, Na₂CO₃ and Na₂O₂, it can be inferred that the functional parts destroying BAM structure are oxoanions, while cations alone can't change the BAM structure. By comparing the BAM reaction behavior with KOH, NaOH, and Ca(OH)₂, BAM structure could be damaged by KOH and NaOH because they can supply free hydroxide ions, while calcium oxide is very stable, and there is no free oxoanion existing in the reaction between BAM and Ca(OH)₂.

Based on the above analysis, a new theory, Free Oxoanion Theory (FOAT), was put forward to summarize the BAM structure decomposition during the alkaline fusion process. FOAT

means that free oxoanions (OH⁻, CO₃²⁻, O₂²⁻) are the key functional group to destroy the BAM structure, while cations alone can't change the BAM structure. A flow diagram illustrating the free oxoanion theory for BAM structure decomposition is shown in Fig. 5. Europium and magnesium ions in BAM are bonded with free oxoanion preferentially to escape from the BAM structure, eventually forming Eu₂O₃ and MgO. The remaining structure of barium aluminate, such as BaAl₁₂O₁₉, is eventually decomposed into aluminate and BaCO₃ in air. Alkali metal cations are introduced to bond with the aluminate ions to maintain the charge balance of the reaction system.

3.3 Lattice energy determination

Lattice energy between different ions was determined by Phil Mann's formula (eqn (3)). Fig. 6 compares the lattice energy results for different substances. In Fig. 6 it can be found that for the same anion, the lattice energy of the substance bonded with the europium ion was always higher than the values for

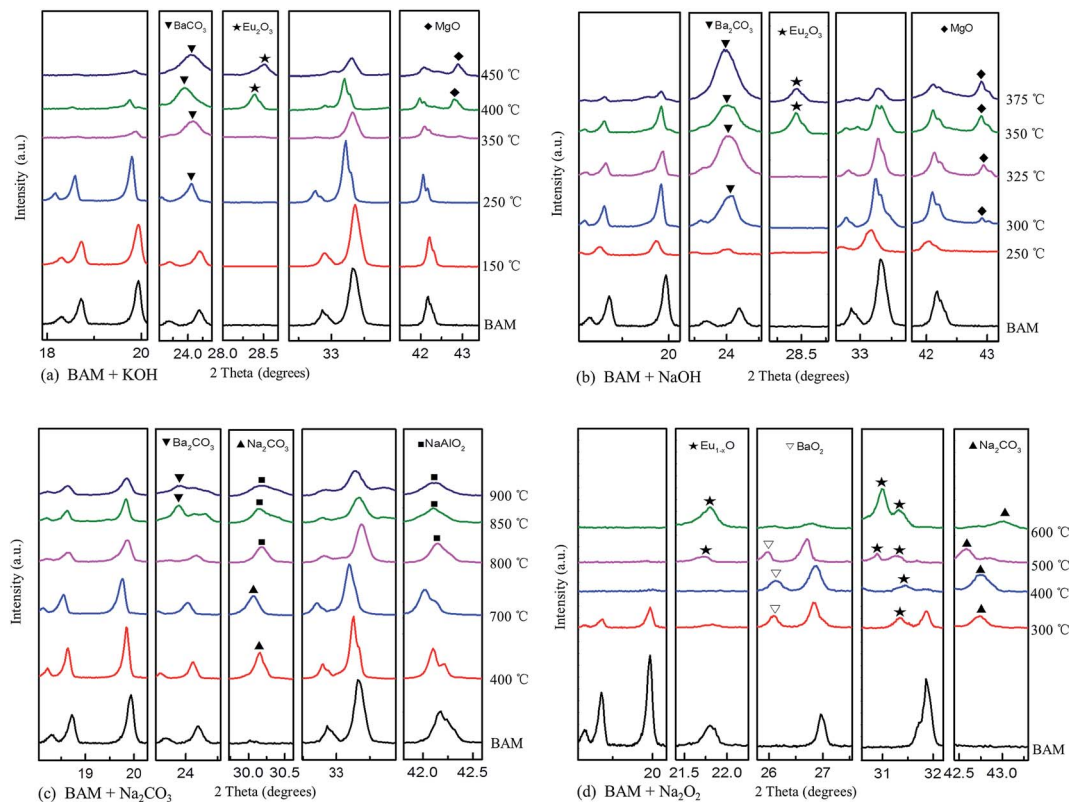


Fig. 3 XRD details of different BAM reactions at different temperature.

magnesium ions, and the values for barium ions were the lowest. Thus, among these three cations, the stability of europium compounds is the strongest, followed by barium, and then magnesium. According to the DSC and XRD results analyzed in Sections 3.1 and 3.2, during the BAM structure damage process, europium ions escape from the structure first,

followed by magnesium and then barium. The reaction order of the BAM decomposition is consistent with the lattice energy calculation results. This demonstrates that the decomposition process of BAM reactions presented in this paper is appropriate.

In Fig. 6, for the same cation, the corresponding lattice energy increased successively for Cl^- , OH^- , CO_3^{2-} , and O^{2-} .

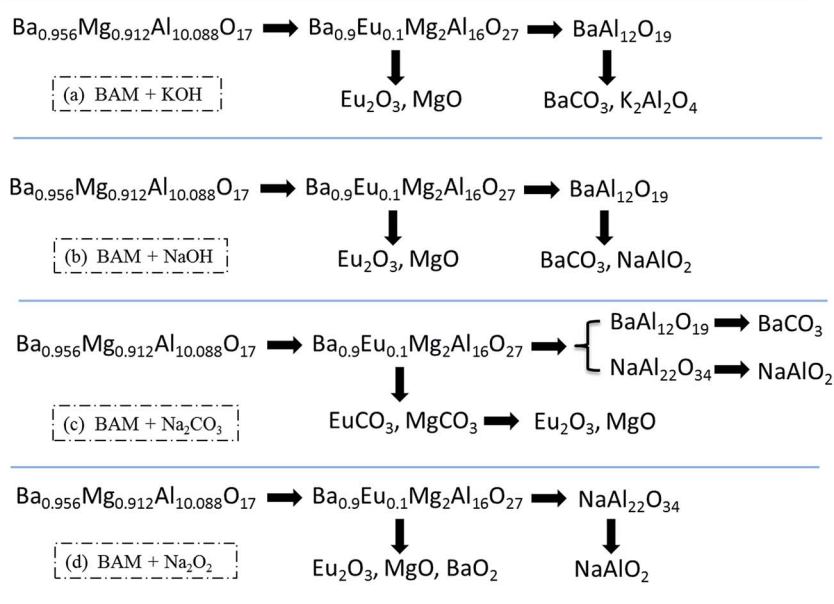


Fig. 4 Flow diagrams of different BAM reactions.

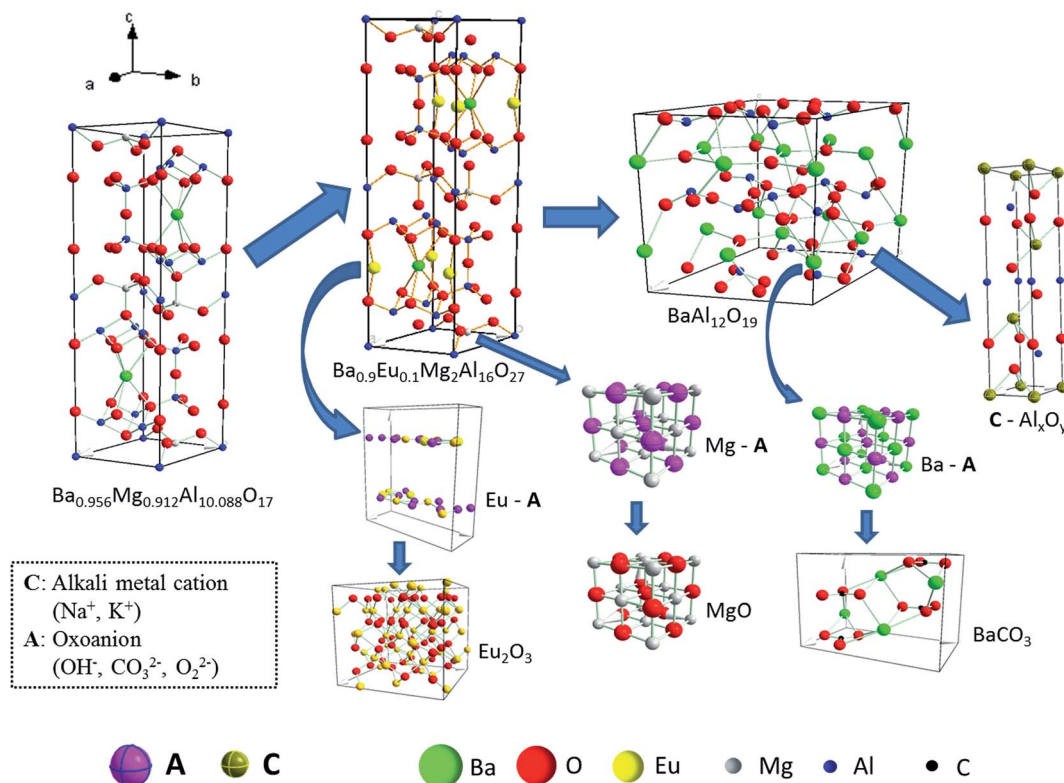


Fig. 5 Summary diagrams of the BAM decomposition process.

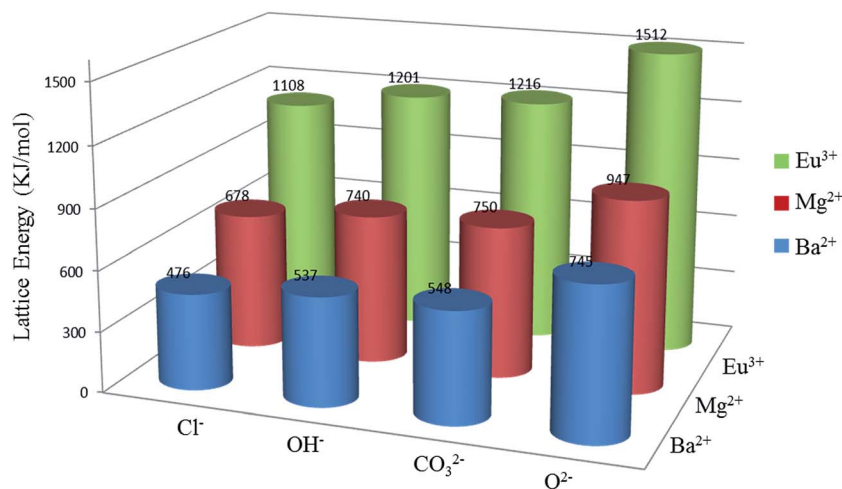


Fig. 6 Lattice energy of different substances bonded with cations and anions.

This indicates that among the substances formed by cations and anions, oxide is the most stable form. During the process of BAM decomposition, Eu/Mg exists as $\text{Eu}_2\text{O}_3/\text{MgO}$. The decomposition temperature of BaCO_3 is about 1450°C , much higher than the studied temperature range, thus Ba eventually formed as BaCO_3 , but not as BaO . The variation of the determined lattice energy is also in agreement with the experimental results, which can explain the ultimate form of the final products during the BAM alkaline fusion process.

4 Conclusions

In this paper, six different reactants (KOH , NaOH , $\text{Ca}(\text{OH})_2$, NaCl , Na_2CO_3 , and Na_2O_2) were chosen to react with BAM to explain the alkaline fusion process. The results presented show that BAM structure could be decomposed to produce new substances by KOH , NaOH , Na_2CO_3 , and Na_2O_2 . By the comprehensive analysis of DSC and XRD, it's clear that BAM alkaline fusion reactions share a similar process. Free Oxoanion

Theory (FOAT) was put forward to elucidate the structure decomposition of BAM. FOAT is described as follows: free oxoanions (OH^- , CO_3^{2-} , O_2^{2-}) are the key functional group to destroy the BAM structure, while cations alone can't change the BAM structure. Europium and magnesium ions in BAM are bonded with free oxoanion preferentially to escape from the BAM structure, eventually forming Eu_2O_3 and MgO . The remaining barium aluminate structure eventually decomposed into aluminate and BaCO_3 in air. Alkali metal cations (Na^+ , K^+) are introduced to bond with the aluminate ions to maintain the charge balance of the reaction system.

For the same cation (Ba^{2+} , Mg^{2+} , Eu^{2+}), the corresponding lattice energy increased successively for Cl^- , OH^- , CO_3^{2-} , and O^{2-} . This variation is in agreement with the experimental phase analysis results, demonstrating that the FOAT summarized in this paper is appropriate. It's a valuable job to recycle REEs from waste phosphors. But due to the lack of a mechanism for the alkaline fusion process, the technology of REEs recycling from waste phosphors is hard to progress. FOAT was summarized to elucidate the BAM structure decomposition, and significantly benefit REEs recycling technology.

Acknowledgements

This project was supported by the National Natural Science Foundation of China (Grants U1360202, 51472030), the National Hi-tech R & D Program of China (Grant no. 2012AA063202), the National Key Project of the Scientific & Technical Support Program of China (Grants no. 2011BAE13B07, 2012BAC02B01 and 2011BAC10B02), the Fundamental Research Funds for the Central Universities (Project no. FRF-TP-14-043A1), the China Postdoctoral Science Foundation Funded Project (Project no. 2014M560885), and the Beijing Nova program (Z141103001814006).

References

- 1 Y. Wu, X. Yin, Q. Zhang, W. Wang and X. Mu, *Resour., Conserv. Recycl.*, 2014, **88**, 21–31.
- 2 K. Binnemans, P. T. Jones, B. Blanpain, T. Van Gerven, Y. Yang, A. Walton and M. Buchert, *J. Cleaner Prod.*, 2013, **51**, 1–22.
- 3 P. K. Tse, *China's rare-earth industry*, US Department of the Interior, US Geological Survey, 2011.

- 4 X. Du and T. E. Graedel, *Environ. Sci. Technol.*, 2011, **45**, 4096–4101.
- 5 C. Yan, J. Jia, C. Liao, S. Wu and G. Xu, *Tsinghua Sci. Technol.*, 2006, **11**, 241–247.
- 6 E. Commission, *Critical raw materials for the EU, Report of the Ad-hoc Working Group on defining critical raw materials*, Technical report, 2010.
- 7 T. Hirajima, K. Sasaki, A. Bissombolo, H. Hirai, M. Hamada and M. Tsunekawa, *Sep. Purif. Technol.*, 2005, **44**, 197–204.
- 8 T. Hirajima, A. Bissombolo, K. Sasaki, K. Nakayama, H. Hirai and M. Tsunekawa, *Int. J. Miner. Process.*, 2005, **77**, 187–198.
- 9 K. Binnemans and P. T. Jones, *J. Rare Earths*, 2014, **32**, 195–200.
- 10 Y. Dong, Z. Wu, X. Han, R. Chen and W. Gu, *J. Alloys Compd.*, 2011, **509**, 3638–3643.
- 11 Z. Chen, Y. Yan, J. M. Liu, Y. Yin, H. Wen, G. Liao, C. Wu, J. Zao, D. Liu and H. Tian, *J. Alloys Compd.*, 2009, **478**, 679–683.
- 12 Y. K. Jeong, H.-J. Kim, H. G. Kim and B.-H. Choi, *Curr. Appl. Phys.*, 2009, **9**, S249–S251.
- 13 K. B. Kim, Y. I. Kim, H. G. Chun, T. Y. Cho, J. S. Jung and J. G. Kang, *Chem. Mater.*, 2002, **14**, 5045–5052.
- 14 H. Liu, S. G. Zhang, D. A. Pan, J. J. Tian, M. Yang, M. L. Wu and A. A. Volinsky, *J. Hazard. Mater.*, 2014, **272**, 96–101.
- 15 Y. Wu, B. Wang, Q. Zhang, R. Li and J. Yu, *RSC Adv.*, 2014, **4**, 7927.
- 16 X. Y. Guo, J. X. Liu, Q. H. Tian and D. Li, *Nonferrous Metals Science and Engineering*, 2013, vol. 4, pp. 6–8.
- 17 G. Bizarri and B. Moine, *J. Lumin.*, 2005, **113**, 199–213.
- 18 Z. H. Wu and A. N. Cormack, *J. Electroceram.*, 2003, **10**, 179–191.
- 19 B. Liu, Y. Wang, J. Zhou, F. Zhang and Z. Wang, *J. Appl. Phys.*, 2009, **106**, 053102.
- 20 S. G. Zhang, H. Liu, D. A. Pan, J. J. Tian, Y. F. Liu and A. A. Volinsky, *RSC Adv.*, 2014, **5**, 1113–1119.
- 21 M. K. Singh, *J. Cryst. Growth*, 2014, **396**, 14–23.
- 22 S. L. Price, *Acc. Chem. Res.*, 2008, **42**, 117–126.
- 23 L. B. Liao and G. Z. Xia, *Crystal Chemistry and Crystal Physics*, Science press, Beijing, 2012, ISBN: 978-7-03-035909-4.
- 24 Y. G. Liang, B. Cheng, Y. B. Si, D. J. Cao, H. Y. Jiang, G. M. Han and X. H. Liu, *Renewable Energy*, 2014, **68**, 111–117.
- 25 R. López-Fonseca, J. R. González-Velasco and J. I. Gutiérrez-Ortiz, *Chem. Eng. J.*, 2009, **146**, 287–294.